(In_{x}Ga_{1−x})_{2}O_{3} alloys for transparent electronics

Hartwin Peelaers, Daniel Steiauf, Joel B. Varley, Anderson Janotti, and Chris G. Van de Walle

(In$_x$Ga$_{1-x}$)$_2$O$_3$ Alloys for Transparent Electronics

Hartwin Peelaers,[1] Daniel Steiauf,[1] Joel B. Varley,[1,2] Anderson Janotti,[1] and Chris G. Van de Walle[1]

[1]*Materials Department, University of California, Santa Barbara, CA 93106-5050, USA*
[2]*Lawrence Livermore National Laboratory, Livermore, CA, USA*

(In$_x$Ga$_{1-x}$)$_2$O$_3$ alloys show promise as transparent conducting oxides. Using hybrid density functional calculations, band gaps, formation enthalpies, and structural parameters are determined for monoclinic and bixbyite crystal structures. In the monoclinic phase the band gap exhibits a linear dependence on alloy concentration, whereas in the bixbyite phase a large band-gap bowing occurs. The calculated formation enthalpies show that the monoclinic structure is favorable for In compositions up to 50%, and bixbyite for larger compositions. This is caused by In strongly preferring sixfold oxygen coordination. The formation enthalpy of the 50/50 monoclinic alloy is much lower than the formation enthalpy of the 50/50 bixbyite alloy and also lower than most monoclinic alloys with lower In concentration; these trends are explained in terms of local strain. Consequences for experiment and applications are discussed.

I. INTRODUCTION

In$_2$O$_3$ can simultaneously exhibit high n-type conductivity and optically transparency.[1] Usually doped with Sn (resulting in indium tin oxide, ITO), In$_2$O$_3$ is the most widely used transparent conducting oxide (TCO), with applications in displays, light-emitting diodes, solar cells, etc.[2] In$_2$O$_3$ has a fundamental band gap of 2.9 eV which is optically forbidden;[3] the onset of absorption occurs almost 1 eV higher. Its crystal structure is cubic bixbyite, with space group 206 (Ia$\bar{3}$), and is shown in Fig. 1(a).

Ga$_2$O$_3$ is a relatively unexplored material, by comparison. In spite of its large band gap of 4.76 eV,[4] high levels of n-type conductivity have been reported, with mobilities up to 150 cm^2/Vs and carrier concentrations exceeding 10^{18} cm^{-3},[5] making the material a candidate TCO in the UV wavelength region.[6] Ga$_2$O$_3$ assumes a monoclinic crystal structure, β-Ga$_2$O$_3$ [Fig. 1(b)], with space group 12 (C2/m), having lower symmetry than bixbyite In$_2$O$_3$.

Ga$_2$O$_3$ has recently come to the forefront because of the ability to grow high-quality material as bulk crystals[7,8] or as thin films by molecular beam epitaxy (MBE).[9,10] Metal-semiconductor field-effect transistors (MESFETs) based on Sn-doped layers grown by MBE on single-crystal substrates were recently reported,[11] as were nanomembrane high-voltage FETs with β-Ga$_2$O$_3$ channels,[12] all attesting to the feasibility of Ga$_2$O$_3$-based electronics.

As in other semiconductor systems, the ability to form heterostructures and alloys would greatly increase the range of potential applications. Alloying Ga$_2$O$_3$ with In$_2$O$_3$ offers an opportunity to tailor the band gap and other properties, and heterojunctions enable electronic and optical confinement. However, the two oxides have very different ground-state crystal structures. It is therefore unclear which structure the alloys would assume, and how this would affect stability and electronic properties. A number of papers have reported on the synthesis of such alloys[14–25] and on their crystal structure, band gaps and solubility limits.
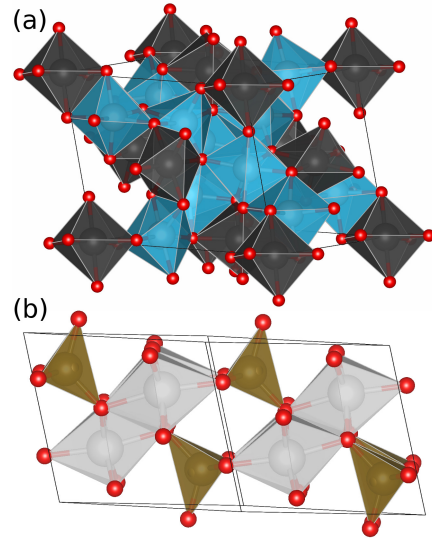
FIG. 1. (Color online) a) Unit cell of bixbyite In$_2$O$_3$, where the symmetric octahedral sites are dark/grey and the distorted site light/blue. b) 1x1x2 supercell of monoclinic Ga$_2$O$_3$, with polyhedra indicating the tetrahedral (dark/brown) and octahedral (light/silver) sites.[13]

However, no consistent explanation for the experimental observations exists.

In this paper we address these issues based on state-of-the-art first-principles calculations to determine formation enthalpies and band gaps of (In$_x$Ga$_{1-x}$)$_2$O$_3$ (InGaO) alloys based on the monoclinic and the bixbyite structures. We explore site preferences, relative structural stability between the bixbyite and monoclinic phases, and optical transitions near the band edge for a series of alloy compositions. Natural band alignments between the parent materials in either structure are reported, which will aid in the design of heterostructures. A number of surprising results are found for alloys. The monoclinic structure is more favorable than bixbyite up to an In concentration of 50%, and the 50/50 alloy in particular has a much lower formation enthalpy than

bixbyite. Band gaps depend strongly on the crystal structure, with bixbyite showing large band-gap bowing and a distinct difference between the fundamental gap and the optical gap (onset of absorption).

II. METHODOLOGY

The calculations are based on density functional theory (DFT) with the projector augmented wave method[26] as implemented in the Vienna Ab Initio Simulation Package.[27] The d states of Ga and In are treated as core states. Traditional DFT functionals lead to large underestimations of the band gap. We therefore use the screened hybrid functional of Heyd, Scuseria, and Ernzerhof (HSE),[28] which mixes the exchange-correlation potential from conventional DFT with exact Hartree-Fock exchange. Hybrid functionals produce more accurate structures and energetics, and the resulting electronic structure is in much better agreement with experiment. The importance of using the hybrid functional in our study is illustrated by the fact that if a traditional semilocal functional is used, Ga_2O_3 is found to be more stable in the bixbyite structure. HSE, on the other hand, correctly predicts the ground-state structure to be monoclinic.

For all HSE calculations presented here, the mixing parameter was fixed to 32%. As shown in Table I, the structural parameters are in very good agreement with experiment. The band gap of Ga_2O_3 is slightly underestimated, while that of In_2O_3 is slightly too large. While it would be possible to adjust the band gap of the pure oxides to the experimental values by choosing an appropriate mixing parameter for each material individually, this is not possible for alloys. The mixing parameter was thus fixed to an intermediate value between In_2O_3 and Ga_2O_3, but this will not affect any of our conclusions.

We use a plane-wave cutoff energy of 500 eV, and the Brillouin-zone integrals are performed on a $4 \times 4 \times 4$ Monkhorst-Pack mesh for the 10-atom cells and a $2 \times 2 \times 2$ mesh for all larger cells, including bixbyite. Convergence checks indicate that the total energy per atom changes by less than 2 meV when the density of the k-point mesh is increased. All calculations are performed at 0 K. The cell shape (angles and ratios of translation vectors) is fixed to that of the stable structures of the parent compounds.

III. RESULTS AND DISCUSSION

A. Band structure and alignment of the binary phases

Figure 2 shows the natural band alignment between the binary compounds in both structures. The band positions were obtained by aligning the thermodynamic $(+/-)$ charge-state transition level of an interstitial hydrogen impurity.[32] The bands were referenced to vacuum

TABLE I. Lattice parameters (for the conventional unit cells), band gaps, and formation enthalpies of monoclinic Ga_2O_3 and bixbyite In_2O_3 as obtained from our calculations and compared with low-temperature experiments.

	monoclinic Ga_2O_3		bixbyite In_2O_3	
	calc.	exp.	calc.	exp.
a (Å)	12.29	12.21[a]	10.21	10.12[d]
b (Å)	3.05	3.04[a]		
c (Å)	5.83	5.80[a]		
β	103.83°	103.83°[a]		
E_{gap} (eV)	4.57	4.76[b]	3.04	2.9[e]
ΔH (eV)	-10.17	-11.29[c]	-8.37	-9.59[c]

[a] Ref. 29.
[b] Ref. 4.
[c] Ref. 30.
[d] Ref. 31.
[e] Ref. 3.

by assuming the $(+/-)$ level to occur at 4.44 eV below the vacuum level. The resulting band positions agree very well (to within 0.04 eV) with results obtained from calculations for the (100) surface of the monoclinic systems, following the methodology described in Ref. 33.

The band gap in the bixbyite structures is direct and located at the Γ point. The monoclinic structures have an indirect gap where the valence-band maximum is 0.04 (0.02) eV higher than the valence-band edge at Γ for Ga_2O_3 (In_2O_3).[34] We observe that the valence-band positions for a given material do not change much between the different crystal phases; the difference in band gap arises mainly from changes in the conduction-band position. The fact that the conduction band in bixbyite lies higher than in the monoclinic phase can be attributed to the higher density (smaller equilibrium volume) of the bixbyite phase, and the absolute deformation potential of an s-orbital-like conduction-band minimum being negative.[35] The valence-band offset between In_2O_3 and Ga_2O_3 is roughly 0.5 eV.

B. Structure and energetics of alloys

We expect that addition of a small amount of In to Ga_2O_3 would preserve the monoclinic structure, and In_2O_3 with a small amount of Ga would maintain the bixbyite structure. In our study we therefore consider ordered InGaO alloys in either the monoclinic Ga_2O_3 structure or the bixbyite structure. The relative stability and formation enthalpy will provide insights into which structures would actually be formed, experimentally.

The primitive 40-atom bixbyite cell of In_2O_3 [Fig. 1(a)] contains 4 cations on symmetric octahedral sites (Wyckoff position 8b) and 12 cations on distorted octahedral sites (Wyckoff position 24d).[31] The monoclinic Ga_2O_3 cell, on the other hand contains 10 atoms with 2 cations on tetrahedral sites (fourfold coordinated with oxygen)
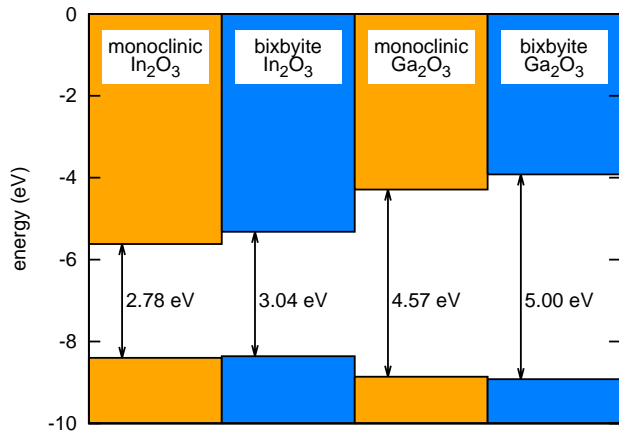
FIG. 2. (Color online) Band alignment between Ga_2O_3 and In_2O_3 in monoclinic and bixbyite structures. The energy zero is the vacuum level.

and 2 on octahedral sites (sixfold coordinated).[29]

For alloys in the monoclinic structure, we use a 1x1x2 supercell [8 cation positions, see Fig. 1(b)], while for alloys in the bixbyite structure we use the primitive cell (16 cation positions). Even then, a complete study of all possible alloy compositions that can be generated is computationally prohibitive. In cases where multiple configurations exist for the same concentration, only the lowest energy configuration is relevant. It was not our purpose to construct a complete thermodynamical model for the alloy, which would require calculations for many more compositions, and at each composition many more configurations. The formation enthalpies obtained here are thus to be considered as upper limits, but our study provides useful insights into the feasibility of alloy formation.

We first examine the lattice parameters. For ease of comparison, we plot the pseudo-cubic lattice parameter, given by the cube root of the volume per formula unit. Figure 3 shows that the InGaO alloys largely follow Vegard's law (the linear interpolation between the binary compounds) for a given crystal structure. The linear behavior is virtually perfect for bixbyite, while for monoclinic small deviations from linearity are observed.

Figure 4 shows the alloy formation enthalpy per cation, defined as

$$\Delta H[(In_xGa_{1-x})_2O_3] = E[(In_xGa_{1-x})_2O_3]$$
$$- (1-x) E[Ga_2O_3] - x E[In_2O_3] , \quad (1)$$

where the monoclinic Ga_2O_3 and bixbyite In_2O_3 structures were taken as the references for the pure phases. For pure In_2O_3, bixbyite has a much lower formation enthalpy than monoclinic, by 690 meV per formula unit. Interestingly, for Ga_2O_3 the monoclinic structure is lower in energy than bixbyite by only 3 meV per formula unit. Indeed, it has already been observed experimentally that Ga_2O_3 readily crystallizes in other phases.[36]

For In concentrations 50% and lower the structures in-
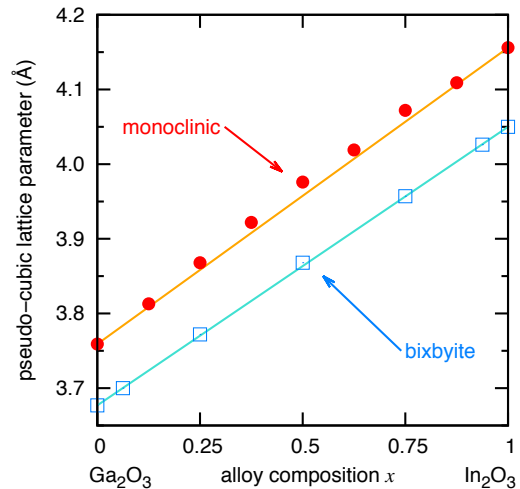
FIG. 3. (Color online) Pseudo-cubic lattice parameter of the lowest energy ordered $(In_xGa_{1-x})_2O_3$ alloys in bixbyite (blue empty squares) and monoclinic (red filled circles) structure. The (orange and turquoise) lines indicate Vegard's law.
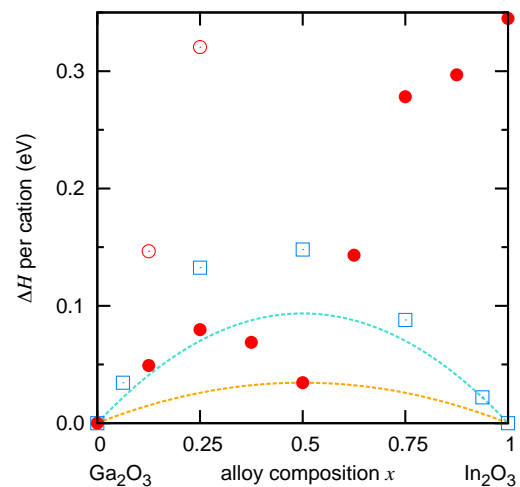
FIG. 4. (Color online) Alloy formation enthalpy [Equation (1)] of ordered $(In_xGa_{1-x})_2O_3$ alloys in the bixbyite (blue empty squares) and monoclinic (red full circles) structure. The hollow red circles are higher energy configurations, as discussed in the text. The parabolas indicate lower limits within the model of Equation (2), with $\Delta H_0 = 35$ meV (orange) and 94 meV (turquoise).

cluded in Fig. 4 all have In atoms occupying only octahedral sites. This result is in agreement with experimental findings on bulk alloys[14,16,17] and, more recently, on InGaO nanocrystals[18] (although in the latter the nanocrystals actually assume the spinel-type γ-Ga_2O_3). This indicates that In on the tetrahedral site is energetically unfavorable. Indeed, configurations where one or two In atoms are located on tetrahedral positions (hollow circles in Fig. 4) are higher in energy than configurations where

all In atoms are located on octahedral sites.

The formation enthalpy of InGaO alloys in the monoclinic structure (circles in Fig. 4) first increases with In concentration, but then decreases when the 50% alloy composition is approached. This can be explained by considering the average In-O bond length in the octahedra: when the 50/50 alloy composition is approached, the average bond length increases, coming closer to the bond length in the bulk bixbyite In_2O_3. This reduces the local strain around the In atom, thereby decreasing the energy. It should be noted that for lower In concentrations, larger supercells could allow for increased local relaxation around the In atoms without putting extra strain on the Ga atoms, so that lower formation enthalpies might be obtained.

For the 50% monoclinic alloy, all octahedral sites are occupied by In and all tetrahedral sites by Ga. Both the In-O and Ga-O bond lengths are close to their respective bulk bond lengths, minimizing the local strain around the atoms. In the 50/50 bixbyite alloy on the other hand, the Ga-O bond lengths in the octahedra are larger than those in the octahedra in bulk Ga_2O_3. This leads to a local strain around the Ga atoms, increasing the formation enthalpy of this structure.

For higher concentrations of In, the formation enthalpy in the monoclinic structure increases sharply. This is because In then necessarily has to occupy tetrahedral sites. Therefore, alloys with In composition greater than 50% will favor the bixbyite structure (squares), while those with compositions 50% and lower will assume the monoclinic structure (circles).

A regular solution model for alloy energetics can be constructed by assuming a parabolic dependence of the enthalpy:

$$\Delta H[(Ga_{1-x}In_x)_2O_3] = 4x(1-x)\Delta H_0 . \quad (2)$$

The parabolas in Fig. 4 are drawn such that the results for monoclinic (or bixbyite) alloys all lie on or above the curves, resulting in ΔH_0=35 meV for monoclinic and 94 meV for bixbyite. We can obtain a lower limit for the temperature T_{mix} at which miscibility is achieved for all concentrations by estimating the mixing entropy of the alloy based on a random mixture,

$$S(x) = -k_B[x \ln x + (1-x)\ln(1-x)] , \quad (3)$$

in which k_B is Boltzmann's constant. The Gibbs free energy G can then be found by $G(x) = \Delta H - TS(x)$. If the temperature is sufficiently high, $G(x)$ will be negative, indicating that mixing is possible. For low temperatures, $G(x)$ has two minima and also a local maximum at $x = 0.5$. The region in between the minima forms a miscibility gap since the free energy of the system will be lowest if the system remains at the compositions given by the location of the minima. If the curvature of G is positive a metastable region with respect to small concentration variations is present. An estimate for T_{mix} can be obtained by requiring that the curvature of $G(x)$

is zero at the local maximum $x = 0.5$. This leads to $T_{mix} = 2\Delta H_0/k_B$. For $\Delta H_0 = 35$ meV (monoclinic), complete mixing is possible at 812 K. This temperature is a lower bound, since it assumes that the completely ordered $x = 0.5$ alloy can be achieved experimentally. Note that already for lower temperatures mixing for small concentrations x is possible.

We can use this model to explain the variation in experimentally reported x values for which a single monoclinic phase was observed. Bulk powder growth techniques typically use temperatures of ~1200°C. These experiments[14,17,20,23] find In concentrations up to $x = 0.43$. In the case of sol-gel growth[25] (900°C), a similar value for x was found. For lower-temperature growth techniques, such as MBE[19] (600°C, x up to 0.35), PLD[21] (650°C, x up to 0.2), and MOCVD[22,24] (700-800°C, x up to 0.25), the obtained concentrations x are lower. A recent theoretical work[37] obtained a solubility limit of x=0.1 at 775-800 K, which is an underestimation of the solubility compared to the experimental results.

The experimental results indicate that the temperature for complete miscibility is likely to be around 900°C = 1173 K, consistent with the fact that our parabolic fit to the enthalpy results in a lower bound. If the temperature is lower than this critical value, a miscibility gap occurs, and a homogeneous alloy can only be obtained for lower x concentrations. Note that the relevant temperature for determining stability of the alloy is the *growth* temperature, not the temperature of device operation. Once the alloys are formed, large kinetic energy barriers prevent decomposition at the operating temperature.

C. Electronic structure of alloys

We now examine the alloy band gap. We will consider the direct band gap at Γ (shown in Fig. 5). Note that the band gap in bulk Ga_2O_3 is indirect, but only 0.04 eV smaller than the direct gap at Γ.[34] In the monoclinic structure, the band gap is close to its linearly interpolated value. In the bixbyite structure, the topmost valence band at Γ in the pure phases is triply degenerate. Symmetry-breaking in the alloys lifts this degeneracy. The average of the three valence bands is far less sensitive to details of atomic structure in the alloy supercells than the individual valence-band energies, similar to previous findings for InGaN alloys.[38] The empty symbols in Fig. 5b represent the band gap corresponding to this average. Distinct bowing is observed, which is conventionally described by the expression

$$E_g[(In_xGa_{1-x})_2O_3]$$
$$= (1-x) E_g[Ga_2O_3] + x E_g[In_2O_3] - bx(1-x) , \quad (4)$$

in which the bowing parameter b is a measure of how far the band gap of the alloy deviates from the linear interpolation between the pure phases. Fitting to the fundamental band gaps in Fig. 5b yields 1.69 eV.
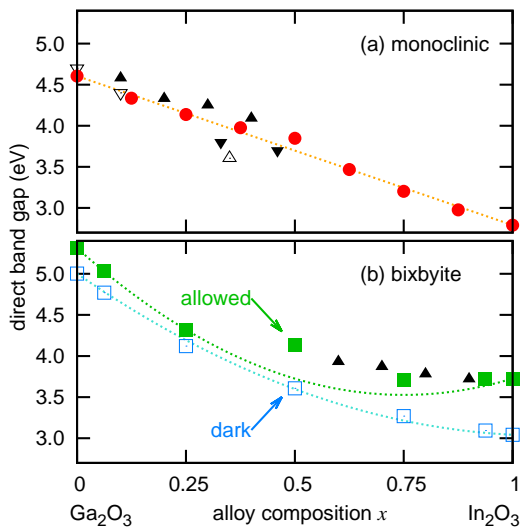
FIG. 5. (Color online) Direct band gap at Γ for ordered $(In_xGa_{1-x})_2O_3$ alloys. a) For the monoclinic Ga_2O_3 structure (red circles), the (orange) line is a linear interpolation between the binary compounds. b) In the bixbyite structure, the empty (blue) squares denote the band gap corresponding to the average of the three highest valence bands; this gap is dark. The lines are the parabolic fit based on Equation (4). The filled (green) squares denote the lowest direct transition at Γ with large dipole matrix element. Experimental values (triangles) are from Refs. 15 (downward open triangles), 19 (downward filled triangles), 24 (upward open triangle), and 20 (upward filled triangles).

Band gaps measured in optical absorption experiments would be higher than this fundamental gap because the transition from the valence-band maximum to the conduction-band minimum is dipole-forbidden at Γ. For pure bixbyite In_2O_3 the onset of strong absorption occurs at 0.7 eV above the fundamental gap. Other transitions (lower in energy) are either also dipole-forbidden or have very small magnitudes (at least 2 orders of magnitude smaller) compared to the strong onset.

The situation is the same for all ordered alloys considered here. The direct transition from the top of the valence band is still forbidden. Optical absorption will only occur at energies corresponding to excitation of an electron from a lower lying valence band with a large dipole matrix element to the conduction-band minimum. The gap corresponding to this large matrix element is shown by the filled symbols in Fig. 5b. These optical gaps exhibit considerable scatter, because the strong transitions at different alloy compositions depend on the character of the valence bands, and this character depends strongly on the specifics of the alloy. Because of this scatter we only fit the parabola to compositions ≤ 0.25, resulting in a bowing of 3.18 eV, which is larger than the bowing for the fundamental gap. Where experimental data are available, they are in good agreement with our calculated band gaps, as shown in Fig. 5. The experimental values

were obtained from absorption[15] and transmission[19,24] spectra and photoelectrochemical measurements.[20]

The information in Fig. 2 can in principle be combined with the data of Fig. 5 to obtain the band edges of InGaO alloys on an absolute scale. Previous results for InGaN alloys[38] indicated that the bowing of the band gap takes place almost exclusively in the conduction band (which reflects different character for different cations), while the absolute position of the alloy valence-band maximum is given by linear interpolation. We expect this rule to hold in the case of InGaO alloys, which are also based on a common anion (whose electronic states make up the valence band).

For transparency in TCOs, it is also important that the energy gap between the lowest and higher-lying conduction bands is sufficiently large, so that free carriers in the conduction band do not lead to direct optical absorption. This gap at Γ is at least 4.1 eV in the ordered bixbyite alloys and 3.5 eV in the ordered monoclinic alloys. A more comprehensive study would be needed to assess whether indirect free-carrier absorption is a concern.[39]

IV. CONCLUSIONS

We have investigated the stability and electronic and structural properties of InGaO alloys using first-principles calculations based on a hybrid functional. Our results indicate that the solubility limit of In in β-Ga_2O_3 is 50%. This can be traced back to the strong preference of In to occupy octahedral sites. The 50/50 monoclinic alloy in particular has a much lower formation enthalpy than the 50/50 bixbyite alloy or than the monoclinic alloys with lower In content, which can be explained by the presence of local strain. Configurations in which In occupies a tetrahedral site are much higher in energy. For In content larger than 50%, we find that the ordered bixbyite structures are more stable than the monoclinic. The band gap strongly depends on the underlying crystal structure, and band-gap bowing is much larger in bixbyite (1.7 eV) than in monoclinic. In bixbyite, we also observe a distinct difference between the optical and fundamental band gaps; for compositions where bixbyite is more stable, this difference is about 0.5 eV.

ACKNOWLEDGMENTS

[1] D. S. Ginley and C. Bright, MRS Bull. **25**, 15 (2000).

[2] O. Bierwagen, Semicond. Sci. Technol. **30**, 024001 (2015).

[3] K. Irmscher, M. Naumann, M. Pietsch, Z. Galazka, R. Uecker, T. Schulz, R. Schewski, M. Albrecht, and R. Fornari, Phys. Status Solidi A **211**, 54 (2014).

[4] T. Matsumoto, M. Aoki, A. Kinoshita, and T. Aono, Jpn. J. Appl. Phys. **13**, 1578 (1974).

[5] E. G. Víllora, Y. Morioka, T. Atou, T. Sugawara, M. Kikuchi, and T. Fukuda, Phys. Status Solidi A **193**, 187 (2002).

[6] N. Ueda, H. Hosono, R. Waseda, and H. Kawazoe, Appl. Phys. Lett. **70**, 3561 (1997).

[7] Z. Galazka, R. Uecker, K. Irmscher, M. Albrecht, D. Klimm, M. Pietsch, M. Brützam, R. Bertram, S. Ganschow, and R. Fornari, Cryst. Res. Technol. **45**, 1229 (2010).

[8] K. Irmscher, Z. Galazka, M. Pietsch, R. Uecker, and R. Fornari, J. Appl. Phys. **110**, 063720 (2011).

[9] T. Oshima, T. Okuno, and S. Fujita, Jpn. J. Appl. Phys. **46**, 7217 (2007).

[10] M.-Y. Tsai, O. Bierwagen, M. E. White, and J. S. Speck, J. Vac. Sci. Technol. A **28**, 354 (2010).

[11] M. Higashiwaki, K. Sasaki, A. Kuramata, T. Masui, and S. Yamakoshi, Appl. Phys. Lett. **100**, 013504 (2012).

[12] W. S. Hwang, A. Verma, H. Peelaers, V. Protasenko, S. Rouvimov, H. G. Xing, A. Seabaugh, W. Haensch, C. Van de Walle, Z. Galazka, M. Albrecht, R. Fornari, and D. Jena, Appl. Phys. Lett. **104**, 203111 (2014).

[13] K. Momma and F. Izumi, J. Appl. Crystallogr. **44**, 1272 (2011).

[14] R. Shannon and C. Prewitt, J. Inorg. Nucl. Chem. **30**, 1389 (1968).

[15] V. I. Vasyltsiv, Y. I. Rym, and Y. M. Zakharko, Phys. Status Solidi B **195**, 653 (1996).

[16] A. F. Pasquevich, M. Uhrmacher, L. Ziegeler, and K. P. Lieb, Phys. Rev. B **48**, 10052 (1993).

[17] D. D. Edwards, P. E. Folkins, and T. O. Mason, J. Am. Ceram. Soc. **80**, 253 (1997).

[18] S. S. Farvid, T. Wang, and P. V. Radovanovic, J. Am. Chem. Soc. **133**, 6711 (2011).

[19] T. Oshima and S. Fujita, Phys. Status Solidi C **5**, 3113 (2008).

[20] A. Kudo and I. Mikami, J. Chem. Soc. Faraday Trans. **94**, 2929 (1998).

[21] H. V. Wenckstern, D. Splith, M. Purfürst, Z. Zhang, C. Kranert, S. Müller, M. Lorenz, and M. Grundmann, Semicond. Sci. Technol. **30**, 024005 (2015).

[22] M. Baldini, D. Gogova, K. Irmscher, M. Schmidbauer, G. Wagner, and R. Fornari, Cryst. Res. Technol. **49**, 552 (2014).

[23] L. Binet, G. Gauthier, C. Vigreux, and D. Gourier, J. Phys. Chem. Solids **60**, 1755 (1999).

[24] F. Yang, J. Ma, C. Luan, L. Kong, and Z. Zhu, in *2011 Symp. Photonics Optoelectron.*, Vol. 3 (IEEE, 2011) pp. 1–5.

[25] Y. Kokubun, T. Abe, and S. Nakagomi, Phys. Status Solidi A **207**, 1741 (2010).

[26] P. E. Blöchl, Phys. Rev. B **50**, 17953 (1994).

[27] G. Kresse and J. Furthmüller, Phys. Rev. B **54**, 11169 (1996).

[28] J. Heyd, G. E. Scuseria, and M. Ernzerhof, J. Chem. Phys. **124**, 219906 (2006).

[29] J. Åhman, G. Svensson, and J. Albertsson, Acta Crystallogr. C **52**, 1336 (1996).

[30] J. A. Dean, ed., *Lange's handbook of Chemistry*, 15th ed. (McGraw-Hill, New York, 1999).

[31] M. Marezio, Acta Crystallogr. **20**, 723 (1966).

[32] C. G. Van de Walle and J. Neugebauer, Nature **423**, 626 (2003).

[33] P. G. Moses, M. Miao, Q. Yan, and C. G. Van de Walle, J. Chem. Phys. **134**, 084703 (2011).

[34] H. Peelaers and C. G. Van de Walle, Phys. Status Solidi B **252**, 828 (2015).

[35] A. Janotti and C. G. Van de Walle, Phys. Rev. B **75**, 121201 (2007).

[36] R. Roy, V. G. Hill, and E. F. Osborn, J. Am. Chem. Soc. **74**, 719 (1952).

[37] M. B. Maccioni, F. Ricci, and V. Fiorentini, Appl. Phys. Express **8**, 021102 (2015).

[38] P. G. Moses and C. G. Van de Walle, Appl. Phys. Lett. **96**, 021908 (2010).

[39] H. Peelaers, E. Kioupakis, and C. G. Van de Walle, Appl. Phys. Lett. **100**, 011914 (2012).